Metrol. Meas. Syst., Vol. 31 (2024) No. 2, pp. 431–449
DOI: 10.24425/mms.2024.149703

METROLOGY AND MEASUREMENT SYSTEMS
Index 330930, ISSN 0860-8229
www.metrology.wat.edu.pl

STABILITY AND PREDICTABILITY OF ZENER REFERENCE VOLTAGE STANDARDS: LONG-TERM EXPERIENCE BY THE LITHUANIAN NATIONAL METROLOGY INSTITUTE

Andrius Bartašiūnas, Rimantas Miškinis, Dmitrij Smirnov, Emilis Urba

Center for Physical Sciences and Technology (FTMC), Saulėtekio Ave. 3, LT-10257 Vilnius, Lithuania
(✉ *andrius.bartasiunas@ftmc.lt*)

Abstract

The Lithuanian national standard of voltage is maintained as the basis for calibration and measurement capabilities of Lithuania published in the Key Comparison Database of the International Bureau of Weights and Measures (BIPM). The stability and uncertainty of the voltage value measurements, performed since 2004 using the calibrated values of the Zener solid-state voltage standards (zeners) to predict their future behavior, are discussed. Conclusions regarding short- and long-term predictability of their behavior, which can be used for choosing an appropriate calibration period, are presented. An estimate of merit for approximations is proposed; based upon the estimate, it is concluded that the hyperbolic approximation is the best one in the most of the cases. Also discussed is the behavior of voltage dividers used in the zeners as well as the recovery of the zeners after a failure of their power supply. It is concluded that the voltage standards operated by the Lithuanian National Electrical Standards Laboratory feature stable drift of the voltage reproduced, which is well predictable by means of linear or non-linear regression.

Keywords: measurement standards, electric voltage, calibration, uncertainty, prediction.

1. Introduction

Clarence Melvin Zener in 1934 proposed a theory describing electrical breakdown of solid dielectrics [1]. The theory has been employed to develop the Zener diodes and solid-state DC voltage standards, which contain the Zener diodes as a voltage reference and include additional circuitry for thermostabilization, generation of other voltages based upon the reference, *etc.* Since late 1980s, the devices called solid-state voltage standards, the Zener reference voltage standards, or simply zeners (we use this term throughout the paper), have been replacing the conventional Weston cell in the capacity of a primary standard of voltage [2, 3]. Nowadays, many *national metrology institutes* (NMIs) use *Josephson Voltage Systems* (JVS) based upon the effect described by Brian David Josephson in 1964 [4] as their national standards. However, as implies a recent

Article history: received November 15, 2023; revised February 23, 2024; accepted February 27, 2024; available online April 4, 2024.

publication [5] as well as some of the calibration and measurement capabilities published at the Key Comparison Database of BIPM, NMIs of some countries still use zeners in this capacity; they are also widely used as transfer and reference standards [6, 7] reproducing stable voltage at fixed values of 10 V and 1.018 V

Since the development of zeners, several commercially available designs with predictable drift of voltage, its low sensitivity to environmental conditions, and high stability have been created. Relative rates of predictable drift of about 10^{-6}/year and relative differences between predicted and measured values as small as $2.5 \cdot 10^{-7}$ have been reported [8].

Much effort is still devoted to the development of new designs of zeners [5,9], assessment of their drift, stability, and sensitivity to ambient conditions [10–12]. On the other hand, research is aimed at improving the properties of the devices, at their statistical assessment and modelling [13–17]. Zeners are used also in other applications, such as heating, temperature sensing, and generation of microwave noise [18, 19]. Also considered are effects of power supply disruptions on the operation of zeners [20].

Because of inevitable drift of voltage reproduced by zeners, they are periodically calibrated against JVS, while the voltage to be reproduced by them after the last calibration is determined by means of prediction based upon the calibration history available. As the calibration is costly, especially when it requires transporting a device abroad, employing the best prediction method (usually, the linear regression is a default choice) and determining the right time for the next calibration is of primary importance.

We describe the behavior from 2004 to 2022 of zeners operated by the *Center for Physical Sciences and Technology* (FTMC) – the Lithuanian NMI – and calibrated regularly against the FTMC's JVS. We consider the results of the regression analysis (both linear and non-linear) of the voltage values reproduced by our zeners, including their predictability using different regression functions and different durations of calibration history. We also attempt to determine the best prediction method and time for the next calibration necessary to ensure the desired prediction accuracy for the voltage values reproduced between calibrations and consider the operation of voltage dividers – deviation of their voltage division ratio from its nominal value.

The Lithuanian national standards of voltage and resistance were developed at the *Electrical Standards Laboratory* (ESL) of FTMC, following the assignment by the Government of the Republic of Lithuania, and were implemented in 2005. The national standard of the electric resistance was described in detail in [21]. The national standard of voltage comprises both primary and secondary standards. The primary voltage standard is made up of a Josephson voltage system, while the secondary standard consists of a group of zeners. The diagram of traceability for DC and AC voltage by means of the direct comparison method is presented in Fig. 1 (AC voltage is out of the scope of this paper).

1.1. Primary voltage standard

ESL's *Josephson Voltage System* (JVS) – a closed-cycle system made by Hypres, USA – is shown in Fig. 2. The array of the Josephson junctions is installed in a vacuum cryostat evacuated by a pump (not shown in the figure) and cooled down to the operating temperature of 4 K by a closed-cycle system, where helium is supplied to the cryo-cooler by a CNA-11 helium compressor. Microwave field necessary for the Josephson phenomenon is provided by a loop of locked frequency made up of a Gunn oscillator, a mixer, a GS1002 power supply-modulator, and an EIP 578B locking microwave counter. Microwave frequency generated by the loop is stabilized using the 10 MHz reference signal coming from the Lithuanian national standard of time and frequency, also operated by FTMC. Microwaves of a selected frequency (usually, it is close to

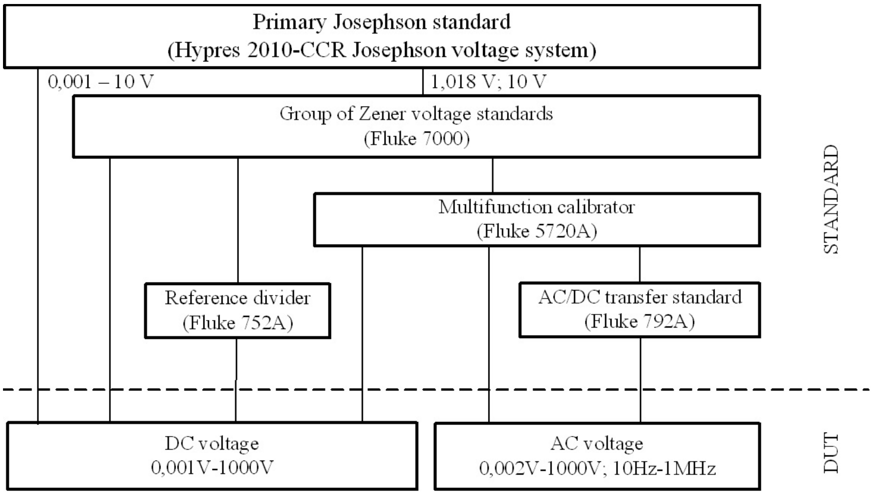

Fig. 1. Traceability of DC and AC voltage in ESL.

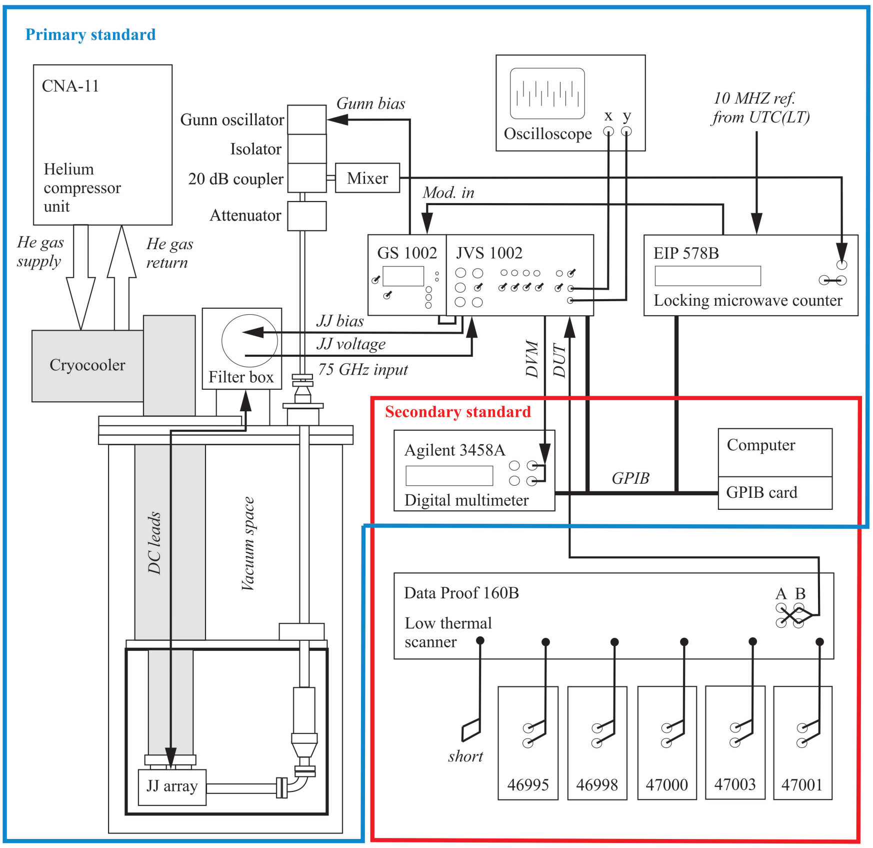

Fig. 2. Calibration setup using the ESL's Josephson voltage system.

75 GHz), within its uncertainty of less than 15 Hz, propagate by the waveguide to the array of the Josephson junctions. Contacts of the Josephson array are connected to the wires, which, through the output filters in a shielded box, are connected to a special connector to which a cable coming from the control unit of JVS 1002 is connected. Via this cable, both the bias and the voltage of the Josephson array are transmitted. Outputs A and B of a Data Proof 160B low thermal e.*m.f. (electromotive force) scanner* in series-opposition are connected to the JVS 1002 through the *device under test* (DUT) cable. An Agilent 3458A digital multimeter connected to the control unit of JVS 1002 is to measure directly the voltage generated by a zener in order to calculate the number of the necessary Josephson step or to operate as a null detector while measuring the difference between voltages of the Josephson array and the zener (this function is enabled by connecting the scanner outputs to the DUT cable in series opposition). For automation of the calibration activities, the devices are connected to the computer via a GPIB interface.

1.2. Secondary voltage standard

The secondary voltage standard consists of a group of five zeners connected to the scanner as well as an Agilent 3458A digital multimeter (DMM) operating as a null detector, which compares the voltages generated by the zeners and the DUT. To this end, the DMM is connected to the scanner having the "Lo" terminals of the scanner's outputs A and B short-circuited and connecting DMM's "Hi" to the terminal "Hi" of the scanner's output B, while DMM's

"Lo" – to the terminal "Hi" of the scanner's output A.

The values of DC voltage at the primary level can be realized in the range of ±10 V At the secondary metrological level, there are five zeners made by *Fluke*, each having fixed value outputs of 10 V and 1.018 V. The output of 10 V is realized by means of transforming the voltage produced by the Zener diode itself, while that of 1.018 V is realized by dividing the 10 V voltage as described in [22]. The traceability to the SI unit of voltage is ensured by calibrating regularly all the five zeners to JVS. Although the values of 10 V and 1.018 V can be realized by the JVS with the relative uncertainty of the order of 10^{-13}, the zeners, due to their internal noise, can be calibrated with the relative uncertainty not better than $5 \cdot 10^{-8}$ and $6 \cdot 10^{-8}$, respectively. Those uncertainties were confirmed by the results of international comparisons in 2005. As well as the above-mentioned JVS, the set of zeners can be used for calibration of DC voltage sources and multimeters at fixed values of 10 V, 1.018 V, and 1 V (see Fig. 1). For this purpose, it is important to know the behavior of each zener, most importantly, its stability.

The output voltage of a zener is affected by ambient temperature, air pressure, and relative humidity. Moreover, voltage values drift due to aging. A zener's sensitivity to environmental conditions and other properties depends on materials and construction chosen by the manufacturer. All the zeners in our set have been manufactured by *Fluke* with their proprietary technology. They feature relative voltage drift of about $8 \cdot 10^{-7}$/year, relative temperature dependence of voltage of about 10^{-6}/K, and relative pressure dependence of voltage of about $2 \cdot 10^{-9}$/hPa, while the humidity dependence is not specified. The influence of ambient temperature is mostly eliminated by the construction of the zeners themselves, where the sensitive chip is placed in a thermostabilized oven. Additional thermostabilization is achieved by keeping ambient temperature in the laboratory room at 23°C ±1°C and relative humidity at 43% ± 10%.

All the *calibration and measurement capabilities* (CMCs) of the Lithuanian NMI in the area of electricity and magnetism now in effect are described in the Key Comparison Database of BIPM [23]. Here, we consider the behavior and prediction of metrological characteristics of the DC voltage standard in the years 2003–2020.

Metrol. Meas. Syst.,Vol. 31 (2024), No. 2, pp. 431–449
DOI: 10.24425/mms.2024.149703

2. Determination of the reference voltage

The calibration of a DUT – *e.g.*, a zener – against the *Josephson Voltage Standard* (JVS) is performed using the NISTVolt software, whose operating principles are outlined below. The basic principle is connecting the JVS and the DUT in series opposition and measuring the difference between the array and DUT voltages with a precision digital voltmeter (DVM) as shown in Fig. 3. The circuit explicitly includes extra signal sources to emulate random noise in the measurement (V_{noise}) as well as thermal voltages existing in the cryoprobe and wiring of the measurement loop together with the zero offset of the DVM and its drift with time – the effects described as $V_o + mt$, where m is the drift rate, and t is the time. An algorithm to eliminate these effects in order to obtain the best estimate of V_{DUT} is used. The measurement is repeated with reversed polarity P to reduce their influence on the measurement furthermore.

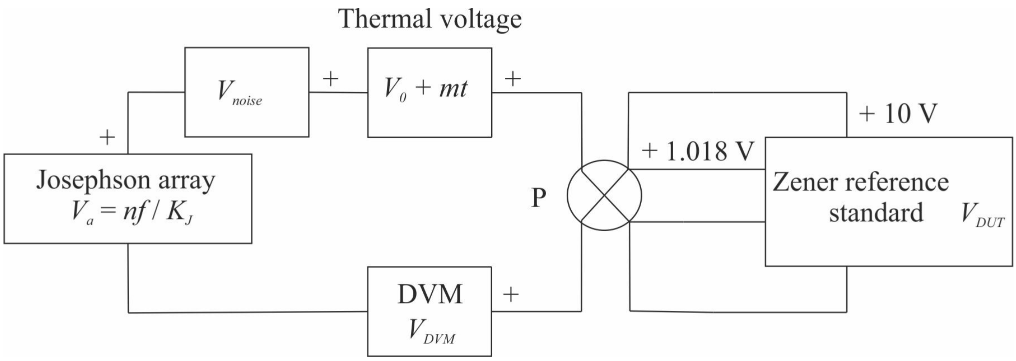

Fig. 3. Measurement circuit including noise, thermal voltages, zero offset of the DVM and its drift, and the reversing switch.

The workflow of the measurement is as follows. At first, the voltage of the Zener reference standard, V_{DUT}, is measured with the DVM to obtain V_e – an estimate of V_{DUT}. Then, the Zener reference standard is connected to the JVS. As it is known, the voltage generated by a Josephson array is described as

$$V_a = nf/K_J, \tag{1}$$

where K_J = 483597.84841698 GHz/V is the Josephson constant, f is the frequency of the driving microwave signal, which is derived from a reference 10 MHz signal generated by the cesium atomic clock of the Time and Frequency Standard Laboratory, and n is an integer step number.

Four sets of measurements are performed – two with the reversing switch in the normal position, that is, $P = +1$, and two with the reversing switch in the reversed position, that is, $P = -1$. Each set consists of ten measurements. After the collection of the first data set, the polarity of the reversing switch is reversed ($P = -1$), and the second set of data is acquired. Two more reversals generate the third and the fourth data sets. Best estimates for V_{DUT}, V_0, and m are obtained from the least-squares regression analysis.

The algorithm used by NISTVolt to calibrate a zener has the following features:

1. The parameter N_{samp} controls the measurement bandwidth by specifying the number of DVM readings to be averaged for each value V_i.
2. Any of about fifty steps near the null point may be used for the measurement.
3. Spontaneous switching between voltage steps during the measurement is tolerated.
4. The DVM and thermal offsets and first-order drifts are fully compensated. However, if the drift exceeds 80 nV/min, the measurement set is rejected and then repeated.

3. History of behavior of ESL's Zener reference voltage standards

Since 2004, the output voltages of all our zeners have been periodically measured using our JVS as described in Section 3; the results are shown in Fig. 4 and summarized in Table 1. The results give a clear hint that the stability of each voltage standard has been different, which may be related to their different sensitivity to environmental conditions, particularly, relative humidity. The standard No. 47003 at its 1.018 V terminal had an almost twice as large drift rate as the others.

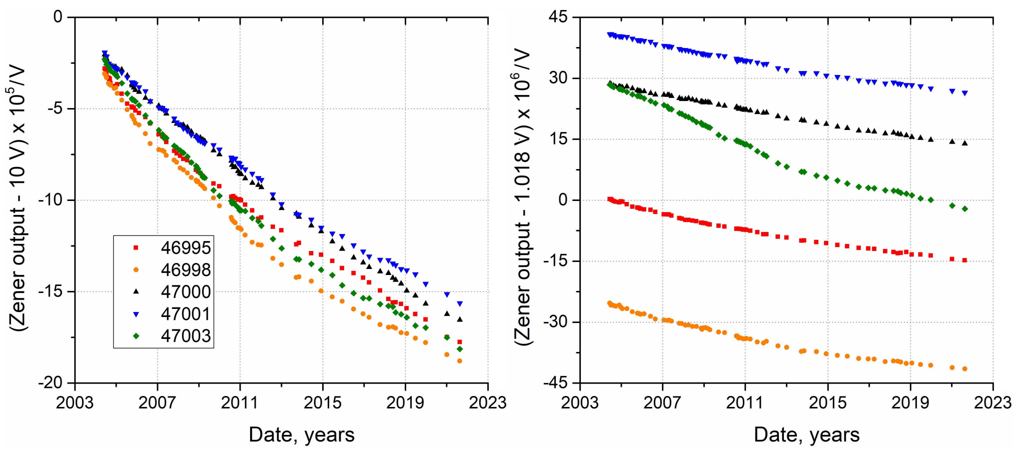

Fig. 4. Output voltages of our zeners at their 10 V terminals (left) and their 1.018 V terminals (right) computed as the session averages. The symbols used for different zeners in the right graph correspond to those used in the left one and are defined in its legend.

Table 1. Drift per year rates of the voltages at the 10 V and 1.018 V terminals of ESL's zeners computed from the results covering the whole period of measurements before the accident, the last four years before the accident, and the period after the accident.

Standard No.	Nominal voltage U_{nom}	Relative drift p_1, (μV/V)/ year, from November of 2004 to March of 2018	Relative drift p_1, (μV/V)/ year, from February of 2014 to March of 2018	Relative drift p_1, (μV/V)/ year, from August of 2018 to January of 2022
46995	10 V	–0.87	–0.59	–0.69
	1.018 V	–0.95	–0.60	–0.56
46998	10 V	–1.00	–0.63	–0.56
	1.018 V	–1.08	–0.60	–0.53
47000	10 V	–0.87	–0.80	–0.69
	1.018 V	–0.88	–0.79	–0.69
47001	10 V	–0.83	–0.64	–0.64
	1.018 V	–0.89	–0.68	–0.67
47003	10 V	–0.99	–0.70	–0.63
	1.018 V	–2.09	–1.14	–1.24

DOI: 10.24425/mms.2024.149703

In July of 2018, an unexpected loss of line power resulted in a discharge of all the batteries of our zeners, and their voltages slightly changed. However, the drift rates have not changed notably. As seen from the graphs, generally, drift rates tend to slightly decrease with time. This trend remains present also after the accident, however, it is not possible to infer whether the trend is less or more pronounced than before. It is clear that the standard No. 47003 at its 1.018 V terminal still features a significantly larger drift rate than the others.

The first-order approach to evaluate the behavior of a zener or another device is the linear approximation of its output parameters obtained by means of linear regression analysis (the least squares method) as

$$U_{\text{approx}} = U_0 + U_{\text{nom}} p_1 t, \tag{2}$$

where U_0 is the value of approximation at the initial moment of time $t = 0$ corresponding to the beginning of measurements, U_{nom} is the nominal voltage of the output considered (10 V or 1.018 V), and p_1 is the relative voltage drift.

Another feature investigated is the stability of the voltage ratio at the two terminals of the zeners. Figure 5 shows the relative deviation of the ratio of the voltages measured at the two terminals from its mean value. The magnitude is defined as:

$$\Gamma = \frac{U_{10\text{ V}}/U_{1.018\text{ V}} - \langle U_{10\text{ V}}/U_{1.018\text{ V}} \rangle}{\langle U_{10\text{ V}}/U_{1.018\text{ V}} \rangle}, \tag{3}$$

where $U_{10\text{ V}}$ and $U_{1.018\text{ V}}$ are the voltages measured at the terminals of a zener at a certain time, while $\langle U_{10\text{ V}}/U_{1.018\text{ V}} \rangle$ is the mean ratio of the voltages obtained throughout all the measurement history. We can see that one of our zeners, S/N 47003, has had a significant drift of the ratio. However, as already mentioned, 1.018 V is produced by dividing the 10 V voltage obtained from the voltage realized by the Zener diode itself. Therefore, the drift of the above ratio does not imply any deviation of the 10 V voltage from its nominal value.

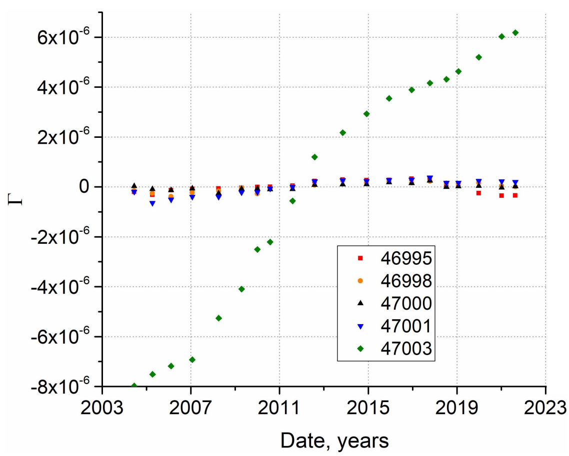

Fig. 5. Relative deviation Γ (defined in (3)) of the ratio of the voltages measured at the two terminals of our zeners from their mean values.

4. Predictability of behavior of the zeners

Predictability of behavior of the zeners as well as that of any other devices is of primary importance because the time period for which it can be predicted within the necessary limits defines the necessary period of calibration. Figures 6 and 7 present estimates of the short- and long-term predictability of the voltage at the 10 V and 1.018 V terminals of our zeners. The estimates have been obtained by taking the calibration results left to a vertical bar representing the cut-off time (the time period denoted as the approximation region on the graphs) and approximating them by the least squares method while using different approximation functions – linear (4), parabolic (5), exponential (6), and hyperbolic (7):

$$U_{\text{approx}} = U_0 + p_1 t, \tag{4}$$

$$U_{\text{approx}} = U_0 + p_1 t + p_2 t^2, \tag{5}$$

$$U_{\text{approx}} = U_0 + a_1 e^{-a_2 t}, \tag{6}$$

$$U_{\text{approx}} = U_0 + b_1/(b_2 + t), \tag{7}$$

where U_0, p_1, p_2, a_1, a_2, b_1, and b_2 are the coefficients of the approximating functions, which are individually determined for every case. Expressions for the coefficients, including those for the linear and hyperbolic function introduced further, are given in Appendix A. Equation (4) is actually the same as (2), rewritten in another form. The magnitude depicted is the relative deviation χ of the actually measured voltage U_{meas} from that given by the approximating function, U_{approx}:

$$\chi = \frac{U_{\text{meas}} - U_{\text{approx}}}{U_{\text{nom}}} \tag{8}$$

versus time. As regards Fig. 6, the calibration history is as long as 15 years, while in the case of Fig. 7, it amounts to 9 years, whereas the time for which the behavior is predicted (the time period denoted as the prediction region on the graphs) is 2 and almost 8 years, respectively. Note that approximating functions were obtained not from all the data obtained before the cut-off time, but only from some of the data points available – roughly one per year. We have excluded a large part of our data set to get closer to the reality of the NMIs which use the zeners as their national standards and cannot afford their frequent calibration against a foreign JVS. On the other hand, we present all the values of relative deviation computed to obtain a better understanding of how adequate our approximations are.

From Fig. 6 describing predictability of the behavior of our zeners at their 10 V terminals for relatively short term (two years), we see that the linear approximation reveals the same trend for all of them, which implies that all of them feature a similar kind of non-linearity, whereas parabolic, exponential, and hyperbolic approximations for different zeners behave differently. Note that the zener No. 47003, which features a drift larger than the others, as indicated by the Table 1, does not feature larger deviation of the output voltage from the approximations. Therefore, its predictability is not worse than that of the others. Non-linear approximations are clearly better than the linear one.

The behavior of the voltage differences at the 1.018 V terminals features the same trends as that of the 10 V ones. Relative differences between the voltage values measured and those predicted are up to 2.5 times larger than those at the 10 V terminals. They are not shown here for brevity.

Now, let's consider the predictability of output voltage of the zeners for relatively long term (8 years) revealed in Fig. 7. The differences between different approximations here are more pronounced. As well as in the short-term case, non-linear approximations are better than the linear one, moreover, those exponential and hyperbolic are more symmetric and generally better than the parabolic one.

DOI: 10.24425/mms.2024.149703

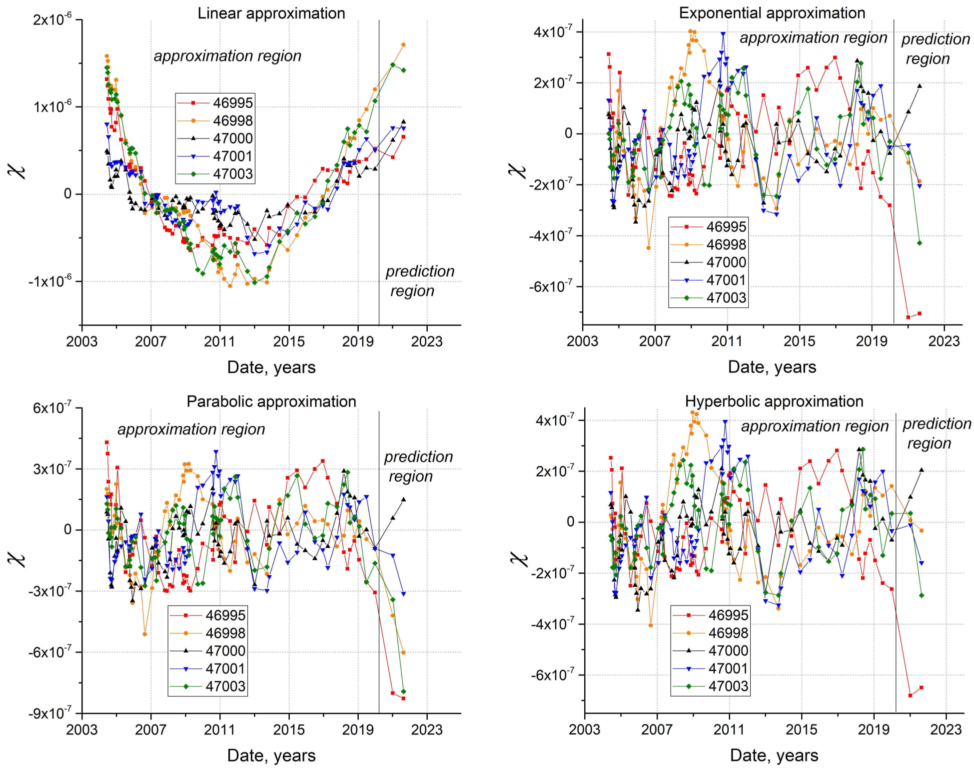

Fig. 6. Short-term predictability of the behavior of our zeners. Relative deviation χ (see (8)) of the actual measured voltage at the 10 V terminals from that given by different approximations defined by (4)–(7).

Once again, the behavior of the voltage differences at the 1.018 V terminals (not shown) features trends similar to those observed at the 10 V terminals and, similarly, is worse than in the case of short-term prediction. Moreover, all the predictions for the 1.018 V terminal of the zener No. 47003, which features a significant drift with respect to the 10 V one (see Fig. 5), are clearly worse than those for the 1.018 V terminals of the others.

After a short disruption of the power supply in July of 2018, due to which the back-up batteries of the zeners had discharged, no tangible changes of the voltage drift rates have occurred, and the accident has had no significant effect on the predictability of the output voltages of the zeners. The results presented by so far, although clearly indicating that approximations do work, do not imply in a straightforward way which method is the best one. It may seem that the curve fitting the measurement results used for approximation in the best way should be expected to predict in the best way also their future behavior, however, in reality, it is not the case. Therefore, we have introduced a magnitude to serve as an estimate of merit for an approximation. We expect it to depend not only on the method and measurement data, but also on the length of the calibration history available and the length of the time period for which the behavior is to be predicted.

We define the magnitude $\sigma(M, N, \tau)$ as

$$\sigma(M, N, \tau) = \sqrt{\frac{1}{R} \sum_{Z=1}^{5} \sum_{p=1}^{k} \sum_{i=1} \{U_{\text{meas}Z}(t_i) - U_{\text{approx}Z,M,N,p}(t_i)\}^2} \tag{9}$$

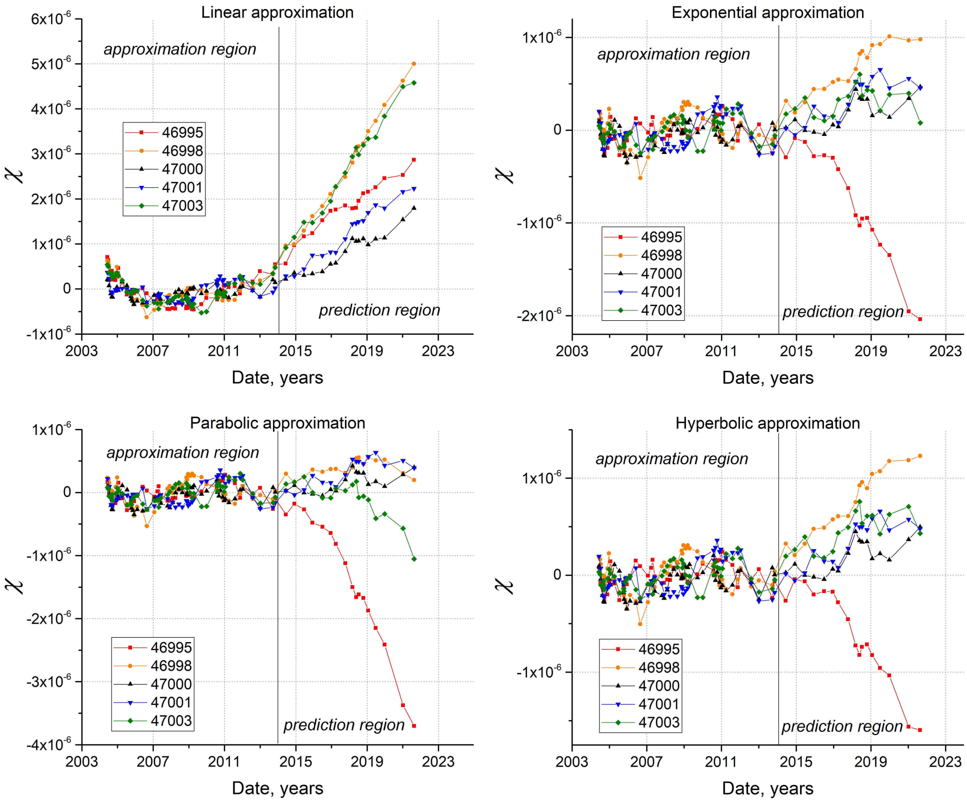

Fig. 7. Long-term predictability of the behavior of our zeners. Relative deviation χ (see (8)) of the actual measured voltage at the 10 V terminals from that given by different approximations defined by (4)–(7).

where $U_{\text{meas}Z}(t_i)$ is the value of voltage measured at the terminals of the Zth zener at time t_i, beginning with the first measurement after the approximation time, t_1, and ending with a point measured roughly time τ after the first point (therefore, summation over i in the last sum is performed while $t_i \leq t_1 + \tau$), whereas $U_{\text{approx}Z,M,N,p}(t_i)$ is the value of voltage predicted by the approximation method M for the Z-th zener at time $t_i$and obtained by taking N yearly measurements, which begin with the p-th one, and R is the number of terms making up the sum. The last point for the medium sum, k, is selected so that there is sufficient time since the end of approximation period till the last measurement available. While computing the last sum, we include all the measurement data available, not only the yearly measurement points. The reduced set of measurements is used only for obtaining the coefficients of the approximating function. In our calculations, we have selected the value of τ to be equal to three years as a reasonable period of time for prediction because it is a longer than usual calibration interval. On the other hand, usually for such a time period the behavior of the zeners can be predicted with an adequate relative accuracy (well below 10^{-6}).

In other words: let's start with, e. g., our first zener and compute the coefficients of the linear regression (let's say, the method number $M = 1$) obtained by taking $N = 4$ yearly measurement points starting with the very first measurement. Then, compute the differences between the values predicted and measured for the time period of about three years starting just after the end of the approximation period and add them in quadrature. Next, compute the linear regression coefficients obtained by taking four yearly measurement points starting with the second measurement and once again compute the differences between the values predicted and measured and add them in quadrature, and so on – until the last point reaches the end of the measurement period – a principle similar to that employed in the Allan and other variances [24]. Finally, repeat the same with the second zener, *etc.*, and also add the differences in quadrature. In this way, we obtain $\sigma^2(1, 4, \tau = 3$ years) as both time and ensemble average. Then, let's take another number of yearly measurement points N and repeat the job; finally, let's take parabolic, exponential approximation, *etc.*, which will allow us to see which method can be expected to yield the best results for the given length of the measurement history. Note that in some cases exponential, hyperbolic, or linear and hyperbolic approximation may not exist as a function with meaningful coefficients.

An algorithm for the calculation of an estimate of merit for the selected approximating method with N yearly measurement points used for approximation, assuming that the number of zeners available is N_Z, is described in Appendix B.

In addition to the four approximating functions for which the prediction results have already been considered, we have introduced one more approximation – linear and hyperbolic one, defined by the van Deemter equation used for fitting the data of experimental gas chromatography [25]:

$$U_{\text{approx}} = U_0 + d_1 t + \frac{d_2}{d_3 + t} \tag{10}$$

where U_0, d_1, d_2, and d_3 are the coefficients of the approximating function. We included it while computing the estimates of merit for the approximation methods. Figure 8 shows normalized estimates of merit for different methods and different number of yearly measurement points used for the approximation (the results were obtained with 10 V terminals). We see that the hyperbolic approximation is the best one in almost all cases, even if the measurement history is short. Even the linear and hyperbolic approximation is not better than the hyperbolic one, however, it may be expected to outperform the others for longer histories of measurement. Linear regression is clearly inferior to all the non-linear estimates if the measurement history is longer than seven yearly measurements. Another inference: if one has a long enough history of yearly calibrations, an ordinary calibration can be postponed for up to three years while still maintaining the relative accuracy of the voltage reproduced at the level of about $3 \cdot 10^{-7}$.

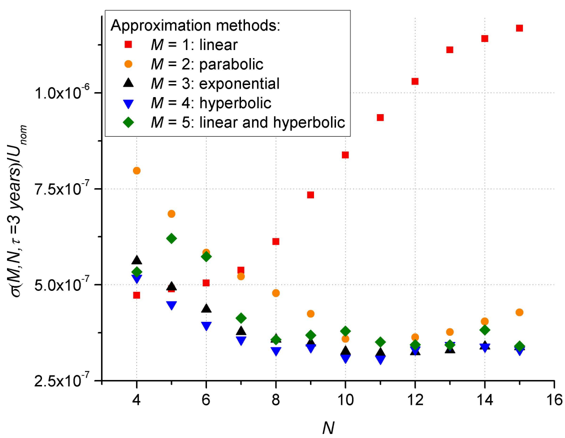

Fig. 8. Normalized estimate of merit $\sigma(M, N, \tau = 3 \text{ years})/U_{\text{nom}}$ for different methods and different numbers of yearly measurement points N used for approximation.

5. Conclusions

The behavior of all our zeners at their 10 V outputs is adequately predictable by means of a linear (if the measurement history is relatively short – containing up to 7 yearly measurements) or nonlinear (in the opposite case) regression. The zener with a drift larger than that of the other devices does not feature predictability worse than that of the others. As far as it can be expected that other zeners of similar type should behave alike, the results obtained imply that, having acquired a reasonably long (about 10 years or longer) history of a single measurement per year and using a hyperbolic or exponential approximation, it is possible to predict the behavior of the zener adequately for several years. An estimate of merit for approximation methods based upon the mean standard deviation of actually measured voltages from their predictions computed for three years since the end of approximation period implies that the hyperbolic approximation is the best one almost in all the cases, except for a history as short as four yearly measurements, when the linear approximation is not inferior to the hyperbolic one. The linear and hyperbolic approximation does not surpass the hyperbolic one for measurement histories available.

The voltages at the 1.018 V terminals, which are produced from 10 V internally, have been stable with respect to the 10 V within ±0.3 ppm, except for the zener featuring a significant drift at the 1.018 V output with respect to the 10 V one. The 1.018 V voltage generated by the zeners is also predictable; however, its prediction accuracy is inferior to that of the 10 V.

Acknowledgements

We would like to thank Prof. Kęstutis Pyragas for a valuable discussion.

References

[1] Zener, C. (1934). A Theory of the Electrical Breakdown of Solid Dielectrics. *Proceedings of the Royal Society A*, *145*(855), 523–529. https://doi.org/10.1098/rspa.1934.0116

[2] Huntley, L. (1987). A primary standard of voltage maintained in solid-state references. *IEEE Transactions on Instrumentation and Measurement*, *IM–36*(4), 908–912. https://doi.org/10.1109/tim.1987.6312580

[3] Spreadbury, P. J. (1991). The ultra-Zener – a portable replacement for the Western cell? *IEEE Transactions on Instrumentation and Measurement*, *40*(2), 343–346. https://doi.org/10.1109/TIM.1990.1032955

[4] Josephson, B. D. (1964). Coupled Superconductors. *Reviews of Modern Physics*, *36*(1), 216–220. https://doi.org/10.1103/revmodphys.36.216

[5] De Souza, H., Trigo, L., & Slomovitz, D. (2021, November). An Ultra Stable Zener Voltage Standard – Fifteen Years of Surveillance. *2021 IEEE URUCON*. 2021 IEEE URUCON. https://doi.org/10.1109/urucon53396.2021.9647064

[6] Slomovitz, D., Landim, R. P., de Souza, H., & Trigo, L. (2023). Bilateral comparison of dc voltage at 10 V between UTE and INMETRO. *Journal of Physics: Conference Series*, *2606*(1), 012029. https://doi.org/10.1088/1742-6596/2606/1/012029

[7] Solve, S., Chayramy, R., & Yang, S. (2018, July). Pressure Sensitivity Coefficients of the BIPM Secondary Voltage Standards. *2018 Conference on Precision Electromagnetic Measurements (CPEM 2018)*. https://doi.org/10.1109/cpem.2018.8501074

[8] Witt, T. J. (2002). Maintenance and dissemination of voltage standards by Zener-diode-based instruments. *IEE Proceedings – Science, Measurement and Technology*, *149*(6), 305–312. https://doi.org/10.1049/ip-smt:20020640

[9] Maruyama, M., Urano, C., Kaneko, N.-H., Yonezawa, T., Kanai, T., Sannomaru, E., Honjot, J., & Yoshino, Y. (2018, July). Investigation of Atmospheric-Pressure Dependence of Compact Detachable Zener Module. *2018 Conference on Precision Electromagnetic Measurements (CPEM 2018)*. https://doi.org/10.1109/cpem.2018.8501195

[10] Stepanov, A., Katkov, A., & Chunovkina, A. (2018, July). Evaluation of Zener Standard Drifts. *2018 Conference on Precision Electromagnetic Measurements (CPEM 2018)*. https://doi.org/10.1109/cpem.2018.8500924

[11] Yang, Y., Meng, J., & Yao, W. (2021). Design of a High-precision 5V/10V DC Voltage Reference Source. *Journal of Physics: Conference Series*, *2087*(1), 012034. https://doi.org/10.1088/1742-6596/2087/1/012034

[12] Maruyama, M., Urano, C., Kaneko, N.-H., Kanai, T., Sannomaru, E., Honjo, J., Tanaka, I., & Yoshino, Y. (2020, August). Investigation of the Influence of Humidity on the Output Voltage of a Prototype of a Compact Detachable Zener Module. *2020 Conference on Precision Electromagnetic Measurements (CPEM)*. 2020 Conference on Precision Electromagnetic Measurements (CPEM 2020). https://doi.org/10.1109/cpem49742.2020.9191792

[13] Bucur, V , Banarie, G., & Marinca, S. (2023, June). Compensation of Temperature Nonlinearity in a Zener-*Based Voltage Reference. *2023 30th International Conference on Mixed Design of Integrated Circuits and System (MIXDES)*. https://doi.org/10.23919/mixdes58562.2023.10203215

[14] Bucur, V , Banarie, G., Marinca, S., & Bodea, M. (2018, June). A Zener-Based Voltage Reference Design Compensated Using a ΔVBE Stack. *2018 25th International Conference "Mixed Design of Integrated Circuits and System" (MIXDES)* (pp. 116–120). IEEE. https://doi.org/10.23919/mixdes.2018.8436687

[15] Champon, X., Angeles, D., Buchheit, T., Canfield, D., Tucker, J. D., & Adams, J. (2023, March 7). A Statistical Assessment of Zener Diode Behavior Using Functional Data Analysis. *2023 7th IEEE Electron Devices Technology & Manufacturing Conference (EDTM)*. (pp. 1–3). IEEE. https://doi.org/10.1109/edtm55494.2023.10103056

[16] Musioł, K., Makowski, P., & Skubis, T. (2015) Coherence investigations of DC voltage group standard. *Bulletin of the Polish Academy of Sciences. Technical Sciences*, *63*(2), 443–448. https://doi.org/10.1515/bpasts-2015-0050

[17] Staniloiu, M.-F., Popescu, H.-S., Rezmerita, G., Vlad, I., & Iordache, M. (2022, October). SPICE model of a real Zener diode tested at room temperature. *International Conference and Exposition on Electrical and Power Engineering (EPE)* (pp. 182–186). IEEE. https://doi.org/10.1109/EPE56121.2022.9959813

[18] McAfee, R., Fish, M., & Gess, J. (2022, May). Zener Diode Reverse Breakdown Voltage as a Simultaneous Heating and Temperature Sensing Element. *21st IEEE Intersociety Conference on Thermal and Thermomechanical Phenomena in Electronic Systems (iTherm)* (pp. 1–5). IEEE. https://doi.org/10.1109/iTherm54085.2022.9899600

[19] Assi, S. A., Omarov, J., & Yıldırım, B. S. (2023). A Novel Microwave Noise Generator Using Multiple Zener Diodes Connected in Series. *IEEE Microwave and Wireless Technology Letters*, *33*(9), 1290–1292. https://doi.org/10.1109/lmwt.2022.3227620

[20] Meléndez, R., Solano, A., & Sánchez, H. (2018, July). Zener DC Voltage Standard Shutdown Behavior. *Conference on Precision Electromagnetic Measurements (CPEM 2018)* (pp. 1–2). IEEE. https://doi.org/10.1109/CPEM.2018.8501099

[21] Bartašiūnas, A., Miškinis, R., Smirnov, D., & Urba, E. (2020). Investigation of the Lithuanian national standard of electric resistance. *Metrology and Measurement Systems, 27*(4), 615–624. https://doi.org/10.24425/mms.2020.134842

[22] Fluke Corporation. (n.d.). *A practical approach to maintaining DC reference standard* [Application Note]. Fluke Digital Library. https://www.elcal.ch/files/11749-eng-01-a.pdf

[23] Key Comparison Database of the BIPM. Calibration and Measurement Capabilities. Electricity and Magnetism, Lithuania.

[24] Barnes, J. A., Chi, A. R., Cutler, L. S., Healey, D. J., Leeson, D. B., McGunigal, T. E., Mullen, J. A., Smith, W. L., Sydnor, R. L., Vessot, R. F. C., & Winkler, G. M. R. (1971). Characterization of Frequency Stability. *IEEE Transactions on Instrumentation and Measurement*, *IM–20*(2), 105–120. https://doi.org/10.1109/tim.1971.5570702

[25] Harris, D. C. (1998). Nonlinear Least-Squares Curve Fitting with Microsoft Excel Solver. *Journal of Chemical Education*, *75*(1), 119. https://doi.org/10.1021/ed075p119

Andrius Bartašiūnas received his M.Sc. degree from Vilnius Gediminas Technical University (VGTU), Lithuania. In the same year, he became an engineer of the Department of Metrology of the Semiconductor Physics Institute, which, after the reorganization in 2010, became part of the Center for Physical Sciences and Technology (FTMC), Vilnius, Lithuania. Currently, he is working in the Electrical Standards Laboratory of FTMC.

Rimantas Miškinis received the Ph.D. degree from the Kotelnikov Institute of Radio-engineering and Electronics (IRE) of the Russian Academy of Sciences (formerly – IRE of the Academy of Sciences of the USSR), Moscow, in 1981. He is currently the head of the two laboratories – Electrical Standards Laboratory and Time and Frequency Standard Laboratory of the Center for Physical Sciences and Technology (FTMC), Vilnius, Lithuania. His research activity focuses on physical metrology, time and frequency measurement technologies, surface acoustic wave devices and sensors.

Dmitrij Smirnov obtained his B.Sc. and M.Sc. degrees in electronics and telecommunications engineering from Vilnius Gediminas Technical University (Vilnius, Lithuania) in 2004 and 2006, respectively. Currently, he is working as a junior research associate at the Department of Metrology of the FTMC (Center for Physical Sciences and Technology, Vilnius, Lithuania).

Emilis Urba received his M.Sc. degree in physics from the Department of Physics of the Vilnius University. After the graduation, he joined the Semiconductor Physics Institute (Vilnius, Lithuania). Since the reorganization in 2010, he has been working as a junior research associate at the Department of Metrology of FTMC (Center for Physical Sciences and Technology, Vilnius, Lithuania). His research interests include acoustics, metrology in the field of time and frequency, and phase noises in oscillators.

Metrol. Meas. Syst., Vol. 31 (2024), No. 2, pp. 431–449
DOI: 10.24425/mms.2024.149703

APPENDIX

A. Expressions for the coefficients of the approximating functions

Assume that we have a set of values $y(i)$ measured at times $x(i)$; $i = 1 \ldots N$. Let's consider approximation of $y(i)$ by means of the least square method using various approximating functions.

1. Linear approximation:

$$f(x) = a + bx. \tag{A.1}$$

From the condition of the minimum mean standard difference between $y(i)$ and the approximation, $\sigma^2 = \frac{1}{N}\sum_{i=1}^{N}(f(x(i)) - y(i))^2$ obtained by zeroing the derivatives of σ^2 with respect to a and b, we obtain the solution. Introducing the following sums:

$$X_1 = \sum_{i=1}^{N} x(i), \quad X_2 = \sum_{i=1}^{N} x^2(i), \quad Y_1 = \sum_{i=1}^{N} y(i), \quad T_{1,1} = \sum_{i=1}^{N} x(i)y(i) \tag{A.2}$$

allows expressing it in a compact form:

$$b = \frac{T_{1,1} - \dfrac{X_1 Y_1}{N}}{X_2 - \dfrac{X_1^2}{N}}, \quad a = \frac{Y_1 - bX_1}{N}. \tag{A.3}$$

2. Parabolic approximation:

$$f(x) = a + bx + cx^2. \tag{A.4}$$

Having employed the same condition with respect to a, b, and c and introduced the sums

$$X_1 = \sum_{i=1}^{N} x(i), \quad X_2 = \sum_{i=1}^{N} x^2(i), \quad X_3 = \sum_{i=1}^{N} x^3(i), \quad X_4 = \sum_{i=1}^{N} x^4(i),$$
$$Y_1 = \sum_{i=1}^{N} y(i), \quad T_{1,1} = \sum_{i=1}^{N} x(i)y(i), \quad T_{2,1} = \sum_{i=1}^{N} x^2(i)y(i), \text{ and}$$
$$Q = \sum_{i=1}^{N} x^2(i) - \frac{1}{N}\left(\sum_{i=1}^{N} x(i)\right)^2 = X_2 - \frac{(X_1)^2}{N} \tag{A.5}$$

we can express c as:

$$c = \frac{N(T_{1,1}X_1X_2 + X_1X_3Y_1) - NQX_2Y_1 - (X_1)^2X_2Y_1 - N^2T_{1,1}X_3 + N^2QT_{2,1}}{2NX_1X_2X_3 - (X_1X_2)^2 - NQ(X_2)^2 - (NX_3)^2 + N^2QX_4}, \tag{A.6}$$

and finally, obtain the values of b and a:

$$\begin{cases} b = \dfrac{1}{Q}\left(\dfrac{cX_1X_2}{N} - \dfrac{X_1Y_1}{N} - cX_3 + T_{1,1}\right) \\ a = \dfrac{Y_1 - bX_1 - cX_2}{N} \end{cases}. \tag{A.7}$$

3. Exponential approximation:

$$f(x) = a + be^{-cx}. \tag{A.8}$$

The solution cannot be found fully analytically. Let's select a positive value of c and compute the sums:

$$X_1 = \sum_{i=1}^{N} e^{-cx(i)}, \quad X_2 = \sum_{i=1}^{N} e^{-2cx(i)}, \quad Y_1 = \sum_{i=1}^{N} y(i), \text{ and } T_{1,1} = \sum_{i=1}^{N} y(i)e^{-cx(i)}. \tag{A.9}$$

Now, we can express corresponding values of b and a using the same expression as in the case of the linear approximation (A.3).

Then, let's compute the derivative with respect to c of the mean standard difference between $y(i)$ and the approximation:

$$\frac{\partial\sigma^2}{\partial c} = \frac{\partial}{\partial c}\frac{1}{N}\sum_{i=1}^{N}\left(a + be^{-cx(i)} - y(i)\right)^2 = -\frac{2b}{N}\sum_{i=1}^{N}\left(a + be^{-cx(i)} - y(i)\right)e^{-cx(i)}x(i). \tag{A.10}$$

Depending on whether $\partial\sigma^2/\partial c$is positive or negative, let's choose another value of c, compute b and a until we find numerically the place where $\partial\sigma^2/\partial c$, while being increasing with increasing c, crosses zero. At this point σ^2assumes its minimum value.

4. Hyperbolic approximation:

$$f(x) = a + \frac{b}{c + x}. \tag{A.11}$$

The solution also cannot be found fully analytically. In the same way as in the case of the exponential approximation, let's select a positive value of c and compute the sums:

$$X_1 = \sum_{i=1}^{N} \frac{1}{c + x(i)}, \quad X_2 = \sum_{i=1}^{N} \frac{1}{(c + x(i))^2}, \quad Y_1 = \sum_{j=1}^{N} y(j)T_{1,1} = \sum_{i=1}^{N} \frac{y(i)}{c + x(i)}. \tag{A.12}$$

Now, we can find corresponding values of b and a using the already considered expression (A.3).

Then, let's compute the derivative of the mean standard difference between $y(i)$ and the approximation with respect to c:

$$\frac{\partial\sigma^2}{\partial c} = \frac{\partial}{\partial c}\frac{1}{N}\sum_{i=1}^{N}\left(a + \frac{b}{c + x(i)} - y(i)\right)^2 = -\frac{2b}{N}\sum_{i=1}^{N}\left(a + \frac{b}{c + x(i)} - y(i)\right)\frac{1}{(c + x(i))^2}. \tag{A.13}$$

Like in the previous case, depending on whether $\partial\sigma^2/\partial c$ is positive or negative, let's choose another value of c, compute b and a until we numerically find the point where $\partial\sigma^2/\partial c$, while increasing with increasing c, crosses zero, and while σ^2assumes its minimum value.

*Metrol. Meas. Syst.,*Vol. 31 (2024), No. 2, pp. 431–449
DOI: 10.24425/mms.2024.149703

5. Linear and hyperbolic approximation:

$$f(x) = a + bx + \frac{c}{d + x}. \tag{A.14}$$

Having selected a positive value of d and computed some more sums than before:

$$X_1 = \sum_{i=1}^{N} x(i), \quad X_2 = \sum_{i=1}^{N} x^2(i), \quad Y_1 = \sum_{i=1}^{N} y(i), \quad T_{1,1} = \sum_{i=1}^{N} x(i)y(i),$$
$$L = \sum_{i=1}^{N} \frac{y(i)}{d + x(i)}, \quad M = \sum_{i=1}^{N} \frac{1}{d + x(i)}, \quad R = \sum_{i=1}^{N} \frac{1}{(d + x(i))^2},$$
$$S = \sum_{i=1}^{N} \frac{x(i)}{d + x(i)}, \quad \text{and} \quad Q = \sum_{i=1}^{N} x^2(i) - \frac{1}{N}\left(\sum_{i=1}^{N} x(i)\right)^2 = X_2 - \frac{(X_1)^2}{N} \tag{A.15}$$

we can express c as:

$$c = \frac{N^2QL + N(MX_1T_{1,1} + SX_1Y_1) - M\,(X_1)^2\,Y_1 - NQMY_1 - N^2ST_{1,1}}{N^2QR + 2NMSX_1 - (MX_1)^2 - NQM^2 - N^2S^2}, \tag{A.16}$$

and compute b and a:

$$\begin{cases} b = \dfrac{1}{Q}\left(\dfrac{cMX_1}{N} - \dfrac{X_1Y_1}{N} - cS + T_{1,1}\right) \\ a = \dfrac{Y_1 - bX_1 - cM}{N} \end{cases}. \tag{A.17}$$

Now, let's compute the derivative of the mean standard difference between $y(i)$ and the approximation with respect to d:

$$\begin{aligned} \frac{\partial\sigma^2}{\partial d} &= \frac{\partial}{\partial d}\frac{1}{N}\sum_{i=1}^{N}\left(a + bx(i) + \frac{c}{d + x(i)} - y(i)\right)^2 = \\ &\quad - \frac{2c}{N}\sum_{i=1}^{N}\left(a + bx(i) + \frac{c}{d + x(i)} - y(i)\right)\frac{1}{(d + x(i))^2}. \end{aligned} \tag{A.18}$$

Like in the two previous cases, depending on whether $\partial\sigma^2/\partial d$ is positive or negative, let's choose another value of c, compute b and a until we numerically find the point where $\partial\sigma^2/\partial d$ while increasing with increasing d, crosses zero, and σ^2 assumes its minimum value.

B. An algorithm for calculation of an estimate of merit for an approximating method defined by (9)

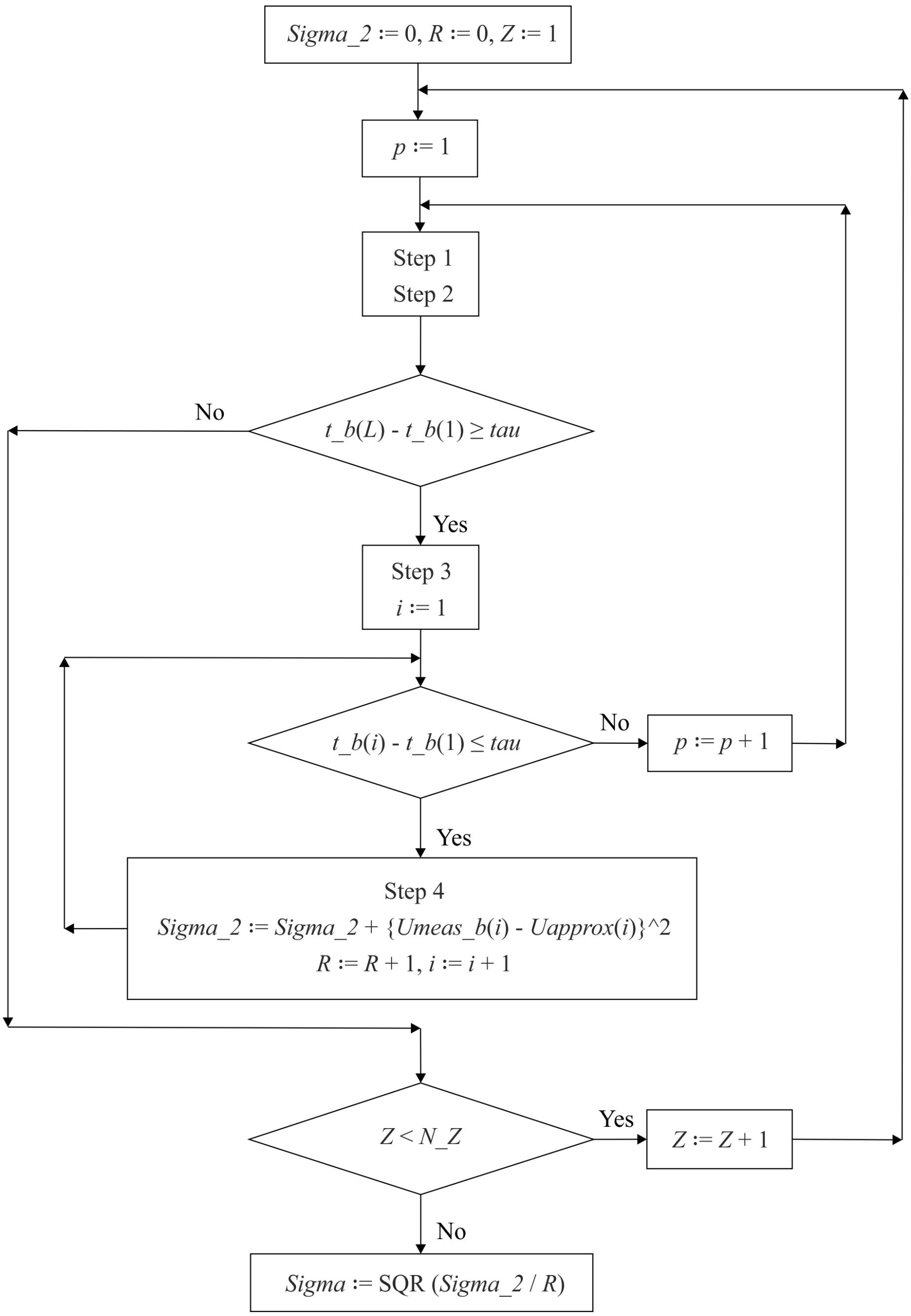

Fig. B.1. Block diagram for the algorithm. Explanations are given further in the text.

General: *Sigma*_2 is the sum of squared differences between the predicted and measured values, R is the counter of the terms of the sum, Z is the number of the zener under consideration, and Z_N is the number of the zeners available.

Step 1: select N yearly measurement points (one measurement per year) starting with the p-th one and obtained by the Z-th zener (note that the value of N cannot be less than the number of constants which define the approximating function). The time period comprising those N yearly measurement times will be referred to as the approximation region. Compose an array $t\_a\,(1\ldots N)$ with their measurement times and an array Umeas_$a\,(1\ldots N)$ with their results.

Step 2: compose an array $t\_b\,(1\ldots L)$ with the measurement times starting with the time of the first measurement after the selected N yearly measurements, $t\_b(1)$, and ending with the time of the last measurement made, $t\_b(L)$. This time period will be referred to as the prediction region. Compose an array Umeas_$b\,(1\ldots L)$ with the corresponding measurement results. The arrays shall include all the measurement results available.

Step 3: from the measurement points of the approximation region stored in the arrays $t\_a\,(1\ldots N)$ and Umeas_$a\,(1\ldots N)$, compute the coefficients of the selected approximating function as described in Appendix A.

Step 4: using the coefficients obtained in Step 3, compute the value assumed by the selected approximating function at the measurement time $t\_b(i)$, Uapprox_i.

The condition $t\_(L) - t\_b(1) \geq tau$ implies that the duration of the prediction region available is not shorter than the time period for which we are going to evaluate the ability of an approximation method to predict the behavior of our zeners. If it is so, we proceed with the calculation of the inner sum of (9), if not – take data of another zener, if that under consideration is not the last one.

The condition $t\_b(i) - t\_b(1) \leq tau$ implies that we are still in the area selected for evaluation of an approximation method. If so, we add the corresponding term to *Sigma*_2, if not – we take the next starting point of yearly measurements by adding 1 to p.

Finally, having processed the data of the last zener available ($Z = Z\_N$), we obtain the mean standard deviation *Sigma* for the selected approximating method, selected number of N yearly measurement points taken for the approximation, and the duration of the prediction time *tau*.